Cancer Cell
Article

Matrix Metalloproteinase-9 Is Required for Tumor Vasculogenesis but Not for Angiogenesis: Role of Bone Marrow-Derived Myelomonocytic Cells

G-One Ahn[1] and J. Martin Brown[1,*]
[1]Division of Radiation and Cancer Biology, Department of Radiation Oncology, Stanford University School of Medicine, 269 Campus Drive, CCSR-South, Room 1255, Stanford, CA 94305, USA
*Correspondence: mbrown@stanford.edu
DOI 10.1016/j.ccr.2007.11.032

SUMMARY

Tumor vasculature is derived from sprouting of local vessels (angiogenesis) and bone marrow (BM)-derived circulating cells (vasculogenesis). By using a model system of transplanting tumors into an irradiated normal tissue to prevent angiogenesis, we found that tumors were unable to grow in *matrix metalloproteinase-9* (*MMP-9*) knockout mice, but tumor growth could be restored by transplantation of wild-type BM. Endothelial progenitor cells did not contribute significantly to this process. Rather, CD11b-positive myelomonocytic cells from the transplanted BM were responsible for tumor growth and the development of immature blood vessels in *MMP-9* knockout mice receiving wild-type BM. Our results suggest that MMP-9 could be an important target for adjunct therapy to enhance the response of tumors to radiotherapy.

INTRODUCTION

Tumor growth depends on the formation of new blood vessels for the supply of oxygen and nutrients through processes known as angiogenesis and vasculogenesis. Angiogenesis occurs primarily by endothelial migration and sprouting from preexisting blood vessels, while vasculogenesis involves the formation of blood vessels in situ by recruitment of precursor cells such as bone marrow (BM)-derived endothelial progenitor cells (EPCs) from the circulation. Although the contribution of EPCs to vasculogenesis has been demonstrated in several models, including hindlimb ischemia (Takahashi et al., 1999), vascular trauma (Gill et al., 2001), and tumor growth (Lyden et al., 2001), the extent to which EPCs are incorporated into newly formed blood vessels in tumors varies significantly with the tumor model (De Palma et al., 2003; Gothert et al., 2004; Lyden et al., 2001).

However, regardless of the different extent of the involvement of EPCs, investigators have commonly observed BM-derived vascular endothelial growth factor receptor-1 (VEGFR-1)-positive myelomonocytic cells associated with the tumor vasculature (De Palma et al., 2003; Lyden et al., 2001). Believed to be derived from a common precursor cell known as the hemangioblast (Rafii et al., 2002), myelomonocytic cells share many characteristics with EPCs. Phenotypically, these cells share a number of surface markers with EPCs, including platelet-endothelial cell adhesion molecule-1 (PECAM-1; CD31), Tie-2, endoglin, and integrate lectin and acetylated low-density lipoprotein (Fujiyama et al., 2003; Rafii et al., 2002; Rohde et al., 2006). Functionally, BM-derived myelomonocytic cells have been shown to mimic EPCs in improving neovascularization in models of normal tissue injury (Capoccia et al., 2006; Fujiyama et al., 2003; Moldovan et al., 2000). These myelomonocytic cells are often observed in the perivascular regions of the endothelium (De Palma et al., 2003; Moldovan et al., 2000) or colocalized with endothelial cells (Bailey et al., 2006; Capoccia et al., 2006; Ruzinova et al., 2003) and have been shown to stabilize the tumor vasculature (Lyden et al., 2001). Moreover, when these cells are depleted either by using the $Id1^{+/-}Id3^{-/-}$ mouse model, where mobilization of VEGFR-1 and VEGFR-2 BM cells are genetically impaired (Lyden et al., 2001), or by using a suicide gene therapy approach (De

SIGNIFICANCE

Tumors have an absolute requirement for neovasculature to grow beyond a very small size. This vasculature can arise by proliferation and migration of nearby blood vessels (angiogenesis) or from colonization by circulating endothelial and other cells primarily derived from the BM (vasculogenesis). Using transplantable tumor models in irradiated tissues (a model that simulates tumors recurring after high-dose radiotherapy), we demonstrate that MMP-9, an enzyme involved in degrading extracellular matrix, is required for vasculogenesis but not for angiogenesis. The BM-derived CD11b-positive myelomonocytic cells expressing MMP-9 are the major contributors to tumor vasculogenesis. This study suggests that MMP-9 from the BM-derived cells could be an important target for adjunct therapy to improve the therapeutic benefit for patients receiving radiotherapy.

Palma et al., 2003), tumor growth is markedly inhibited. Overall, these studies indicate that BM-derived myelomonocytic cells play an important role in tumor vasculogenesis.

The BM-derived myelomonocytic cells that infiltrate tumors and differentiate into macrophages are commonly referred to as tumor-associated macrophages (TAMs). Clinical evidence indicates that the presence of large numbers of TAMs correlates with poor prognosis in cancers (Pollard, 2004). TAMs are a polarized population of macrophages (Sica et al., 2006) and release many angiogenic factors, including vascular endothelial growth factor (VEGF), interleukin-8, tumor necrosis factor-α, and matrix metalloproteinase-9 (MMP-9) (Dirkx et al., 2006; Lewis and Pollard, 2006; Yang et al., 2004).

MMP-9 is a member of a family of zinc-containing endopeptidases that is involved in degradation of extracellular matrix (ECM) and in vascular remodeling (Heissig et al., 2003). Like other members of the MMP family, MMP-9 is synthesized as an inactive zymogen (pro-MMP-9) that is activated by proteolysis or autolysis (Bergers and Coussens, 2000; Galis and Khatri, 2002). MMP-9 is involved in mobilizing EPCs and other progenitor cells from the BM niche (Heissig et al., 2002), liberating growth factors including VEGF (Bergers et al., 2000) and transforming growth factor-β (Yu and Stamenkovic, 2000) from the matrix-bound forms, and recruiting the BM-derived leukocytes to the tumor vasculature (Jodele et al., 2005). MMP-9 provided by BM-derived cells has been shown to initiate the angiogenic switch leading to tumor growth and progression in K14-HPV16 epithelial squamous carcinoma in mice (Coussens et al., 2000; Giraudo et al., 2004).

Radiotherapy is one of the most important treatment modalities for cancer. However, many patients treated with radiotherapy relapse in the irradiated field (Liang et al., 1991). It is unclear how this occurs because, even though all of the tumor cells may not be killed by radiation, it is unlikely that a sufficient number of endothelial cells to allow for subsequent tumor growth could survive the large doses delivered in radiotherapy (Itasaka et al., 2007; Tsai et al., 2005). One possibility to account for this is that a subset of BM-derived cells could enter the irradiated tumor and restore the vasculature by vasculogenesis. EPCs have recently been shown to rescue tumor growth following treatment by vascular disrupting agents (Shaked et al., 2006), but it remains to be determined whether this could also apply following irradiation.

In the present study we investigate the role of the BM-derived CD11b-positive (CD11b+) myelomonocytic cells expressing MMP-9 in the growth of tumors that are irradiated or transplanted into a tissue that has been irradiated prior to transplantation. Tumors grown in previously irradiated tissues generally show an increased latency period and a reduced growth rate because of impaired neovascularization resulted from radiation-induced injury to the host vasculature and connective tissue (a phenomenon known as the "tumor bed effect") (Milas et al., 1986). Such tumors also have an increased metastatic potential, reduced blood perfusion and oxygen tension, and resistance to treatments such as ionizing radiation and cytotoxic agents, thereby mimicking human primary tumors that recur following radiotherapy (Rofstad et al., 2005). We therefore hypothesized that the vasculature of tumors grown in previously irradiated tissues would derive from cells circulating in the blood stream and in particular the BM. We show that tumors did not grow in preirradiated subcutaneous tissues of *MMP-9* knockout (KO) mice and that MMP-9 expressing CD11b+ myelomonocytic cells in the tumors from transplanted BM cells restored tumor growth in these mice. We further provide evidence that MMP-9 expressing BM-derived myelomonocytic cells are essential to the process of vasculogenesis and could be an important target for adjunct therapy to high-dose radiotherapy.

RESULTS

BM-Derived Cells Infiltrating Tumors Are Not EPCs

We examined the BM-derived infiltrates in MT1A2 mouse mammary carcinoma in FVB mice or radiation-induced fibrosarcoma (RIF) in C3H mice by in situ hybridization for a Y-specific DNA probe in female mice that had received syngeneic male BM cells. Consistent with the fact that both the MT1A2 (Guy et al., 1992) and RIF (see Experimental Procedures) tumors are of female origin, we found no staining for the Y-probe in these tumors grown in female mice (Figure 1A). However, when grown in female mice transplanted with male BM, we saw significant infiltration of male-derived cells that was different for the two tumors: MT1A2 tumors showed BM-derived infiltrates mainly in perivascular regions, whereas RIF tumors showed a more diffusely distributed pattern (Figure 1A).

Because the dose of irradiation (IR) used in this study (20 Gy) would be expected to sterilize essentially all of the endothelial cells in the irradiated tissue prior to tumor transplantation and hence abrogate local angiogenesis (Udagawa et al., 2007), we hypothesized that the BM-derived infiltrates may be EPCs and that the tumors grown in the irradiated bed might incorporate more EPCs from the BM to establish the tumor vessels by vasculogenesis. First, we examined whether 20 Gy of IR to subcutaneous tissues of the lower back of the mice would cause ulceration to the skin. We found that there was no difference in the histology of the skin between irradiated and nonirradiated mice (Figure S1A available online) and that there were infiltrating cells present only when the tumor was implanted on the irradiated skin (Figure S1B). We therefore quantified the BM-derived EPCs in MT1A2 tumors grown in the preirradiated tissues ("pre-IR bed") of mice that had received BM cells from *Tie2*lacZ transgenic mice, which express the *lacZ* reporter gene driven by the endothelial receptor tyrosine kinase promoter *Tie2* (Schlaeger et al., 1997). EPCs were detected by double-label immunostaining for X-gal and CD31. The growth kinetics showed that tumors grew significantly slower in preirradiated tissues (Figure 1B and Figure S3), as reported by others (Milas et al., 1986; Rofstad et al., 2005). We confirmed that Tie2 marks endothelial cells in MT1A2 tumors by growing the tumors in *Tie2*-lacZ transgenic mice (Figure 1C). However, when grown in mice that had received BM cells from *Tie2*lacZ mice, the tumors showed only rare incorporation of EPCs in the vessels (Figure 1C). Tumors grown in preirradiated tissues of these BM transplanted mice also showed very low levels of EPCs in the tumor vasculature (Figure 1C), and the proportion of CD31 and X-gal double-positive tumor vessels did not differ significantly between control tumors without IR and tumors grown in preirradiated tissues (Figure 1C). However, in the tumors grown in preirradiated tissues we observed a significant number of Tie2-expressing cells in stromal regions of the tumors that were not positive for CD31 staining (Figure 1D).

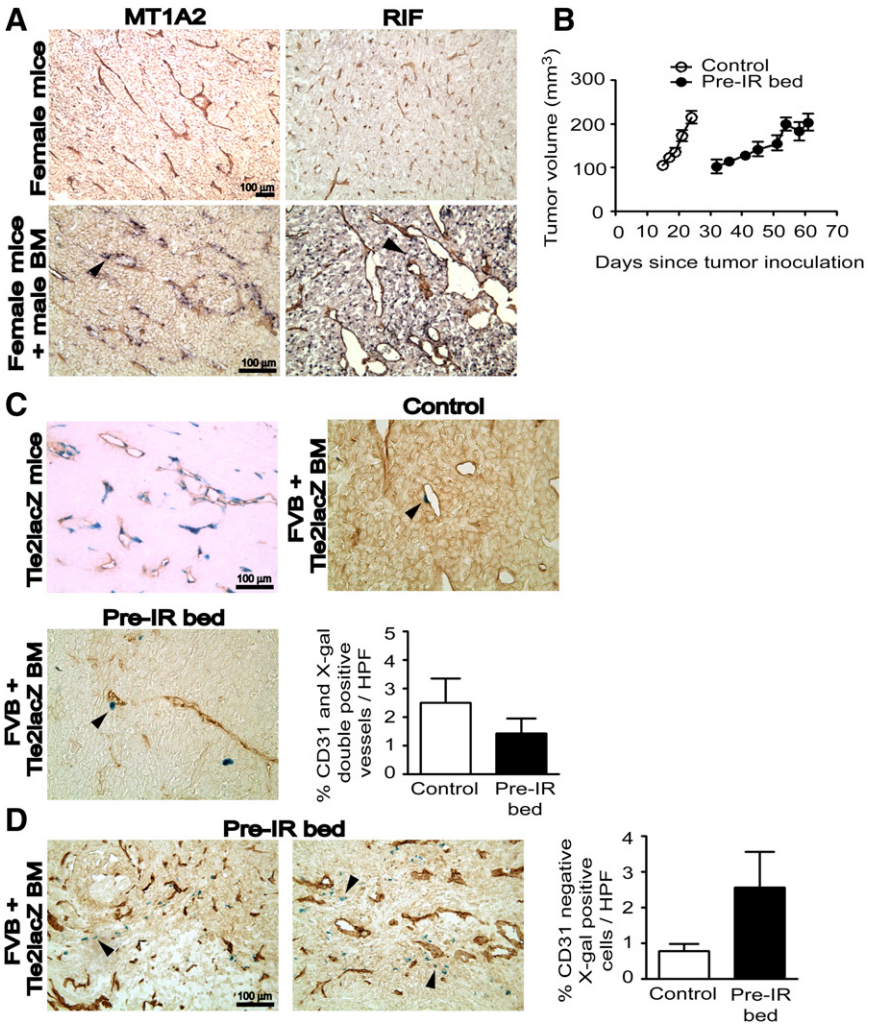

Figure 1. BM-Derived EPCs Contribute Minimally to Tumor Vasculogenesis

(A) MT1A2 and RIF tumors grown in female mice (upper panel) or in female mice that had received syngeneic male BM cells (lower panel). The tumors were stained for CD31 (brown) and Y-DNA probe by in situ hybridization (dark blue). Arrowheads (black) in the lower panel indicate cells positively stained for the Y-probe.

(B) Growth kinetics of MT1A2 tumors grown in nonirradiated (control; open symbols) or preirradiated (pre-IR bed; filled symbols) subcutaneous tissues of FVB mice.

(C) MT1A2 tumors grown in *Tie2*lacZ transgenic mice (Tie2lacZ mice) or in FVB mice that had received BM cells from *Tie2*lacZ mice (FVB + Tie2-lacZ BM). Tumors in FVB + Tie2lacZ BM were grown in nonirradiated (control) or preirradiated (pre-IR bed) tissues. Vessels were stained with CD31 (brown) and X-gal (blue). Arrowheads (black) indicate some of the BM-derived LacZ-positive cells. The graph shows quantification of CD31- and X-gal-double-positive vessels cells as a percentage of the total CD31-positive cells in high power field (HPF). The difference between control and pre-IR bed was not statistically significant ($p > 0.05$).

(D) A significant number of X-gal (blue)-positive but CD31 (brown)-negative cells were observed in the tumors grown in the preirradiated tissues (pre-IR bed) of FVB + Tie2lacZ BM (indicated with black arrowheads). Quantification of X-gal-positive but CD31-negative cells counted per HPF is shown on the right. The data were not, however, significantly different between control and pre-IR bed ($p > 0.05$).

Symbols and error bars in (B), (C), and (D) are the mean ± SEM for $n \geq 5$ mice per group.

To determine if the minimal incorporation of BM-derived EPCs in the tumors was a general phenomenon, we examined a number of different tumor models: TG1-1 mouse mammary carcinoma or 6780 lymphoma in FVB mice with BM cells from *Tie2*lacZ mice; and the Lewis lung carcinoma (LLC) or B16F1 melanoma in C57Bl/6 with BM cells from either *Tie2*GFP or *Rosa26* transgenic mice. Double-label immunostaining for BM-derived EPCs again showed that there was only rare incorporation of EPCs in the tumor vasculature of all control tumors and tumors grown in preirradiated tissues (Figure S2).

Overall, the results suggest that BM-derived EPCs contribute only to a small extent to tumor blood vessels and that they are not a major component of the BM-derived infiltrates in the tumors used in this study.

CD11b+ Myelomonocytic Cells Account for Most of the BM-Derived Infiltrates in the Tumors and Are Increased by IR

To ascertain the nature of the BM-derived infiltrates in the tumors, we examined MT1A2 tumors grown in preirradiated tissues of mice that had received BM cells from mice ubiquitously expressing green fluorescent protein (GFP). The GFP-expressing BM-derived infiltrates in the tumors were examined for markers of inflammatory cells including cytotoxic T cells (CD8α), helper T cells (CD4), natural killer cells (CD49b), monocytes/macrophages (CD11b), dendritic cells (CD11c), and granulocytes/neutrophils (Gr-1). Double-label immunofluorescent staining showed that a significant number of GFP-expressing cells colocalized with CD11b (Figure 2A). Although there were some CD4- or CD8α-positive cells detected in the tumors, they did not colocalize with GFP (Figure 2A), indicating that these cells are not derived from the BM but possibly from the thymus or spleen. We did not observe any detectable numbers of CD11c-, Gr-1-, or CD49b-positive cells in the tumors that were also positive for GFP (Figure 2A).

We next determined how the BM-derived CD11b+ myelomonocytic cells in the tumors were affected by IR. Tumors were grown either without IR (control) or in preirradiated tissues (pre-IR bed) as previously. We also tested a clinically relevant IR model by delivering a single dose of IR (20 Gy) to already established tumors at approximately 200 mm^3 and allowing the tumors to regrow beyond the volume at which they were irradiated (IR tumor). Immunostaining showed that both IR tumors and tumors grown in preirradiated tissues had significantly more CD11b+ cells compared to control MT1A2 tumors of the same size (Figures 2B and 2C). In RIF tumors, we also observed more CD11b+ cells in the IR tumors, although tumors grown in

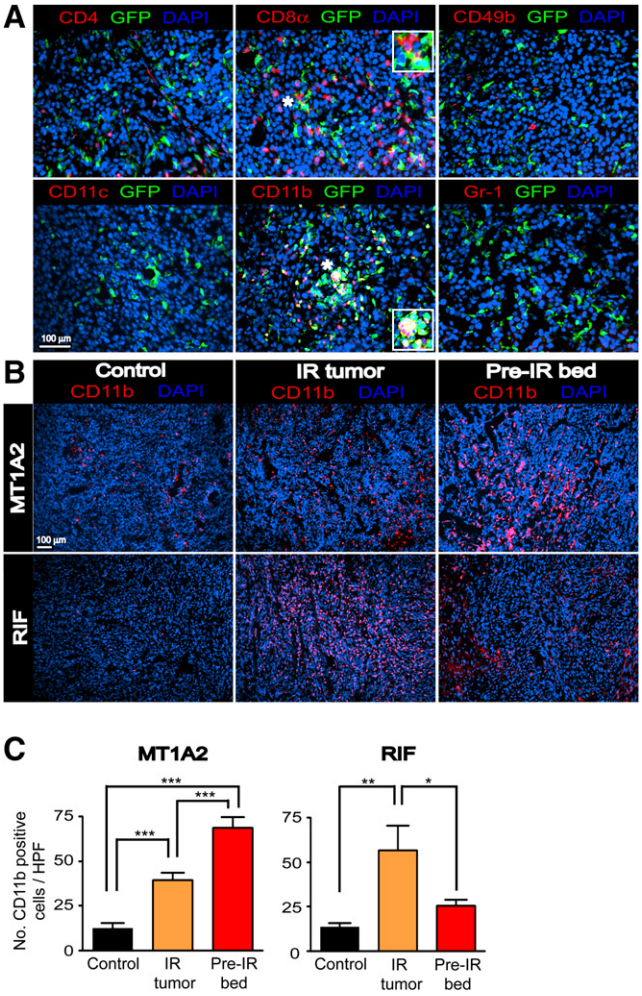

Figure 2. BM-Derived CD11b+ Myelomonocytic Cells Are Recruited to the Tumors with IR

(A) Immunostaining of MT1A2 tumors grown in the preirradiated tissues of FVB mice that had received BM cells from mice ubiquitously expressing GFP. Tumor sections were stained for CD4 (red), CD8α (red), CD49b (red), CD11c (red), CD11b (red), or Gr-1 (red), and anti-GFP (green), counterstained with DAPI (blue). Colocalization of red, green, and blue is shown in white. Insets in the middle panels show magnified regions of the microphotograph where indicated with asterisks.

(B) Immunostaining for CD11b (red) in tumors with no IR (control), irradiated tumors (IR tumor), or tumors grown in the irradiated bed (pre-IR bed) for MT1A2 (upper panel) and RIF (lower panel). Nucleus staining with DAPI is shown in blue.

(C) Quantification of CD11b+ myelomonocytic cells in (B) for MT1A2 (left) and RIF (right) tumors. Symbols and error bars represent the mean ± SEM for $n \geq 4$ animals per group. *$p < 0.05$, **$p < 0.01$, and ***$p < 0.001$, respectively, determined by one-way ANOVA.

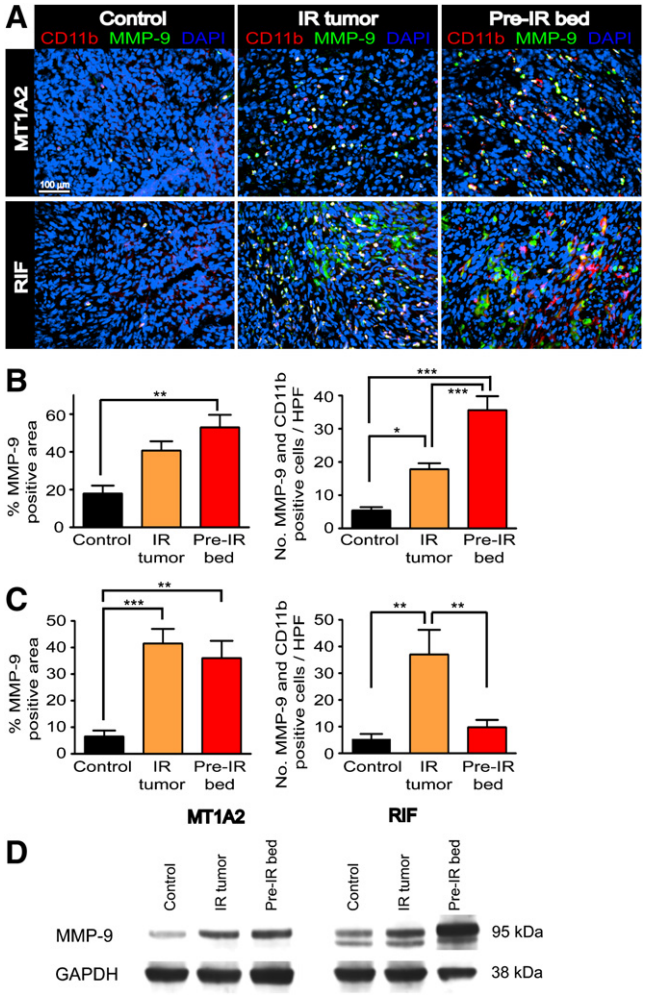

Figure 3. CD11b+ Myelomonocytic Cells Express MMP-9 in the Tumors

(A) Double-label immunofluorescent staining for CD11b (red) and MMP-9 (green) in MT1A2 (upper panel) and RIF (lower panel) tumors with no IR (control), irradiated tumors (IR tumor), or grown in preirradiated tissues (pre-IR bed). Colocalization of CD11b and MMP-9 is shown in white with DAPI counterstaining.

(B) Quantification of MMP-9-positive area determined by the point-count method (left) and the number of CD11b- and MMP-9-double-positive cells in nonnecrotic regions (right) of MT1A2 tumors.

(C) RIF tumors as in (B). Symbols and error bars in (B) and (C) are mean ± SEM for $n \geq 4$ animals per group. *$p < 0.05$, **$p < 0.01$, and ***$p < 0.001$, respectively, by one-way ANOVA.

(D) Western blot for MMP-9 in MT1A2 (left panel) and RIF (right panel) tumors. GAPDH was used as the loading control.

preirradiated tissues showed similar numbers of CD11b+ cells to controls (Figures 2B and 2C). The latter was because there were only small proportions of viable cells present in RIF tumors grown in preirradiated tissues.

CD11b+ Myelomonocytic Cells Express MMP-9

Because of the known role of monocytes/macrophages in promoting tumor angiogenesis (Coussens et al., 2000; Giraudo et al., 2004; Lin et al., 2006) we hypothesized that CD11b+ myelomonocytic cells contribute to the vasculogenesis of the tumors grown in the irradiated bed by remodeling the ECM. We tested this hypothesis by examining the expression of MMP-9, one of the key players in remodeling ECM, in CD11b+ cells using double-label immunofluorescent staining. Histological examination showed that most of the CD11b+ cells were also MMP-9 positive in MT1A2 tumors (Figure 3A). Moreover, irradiated tumors (IR tumors) and tumors grown in the irradiated bed (pre-IR bed) showed an increase in MMP-9-positive areas and

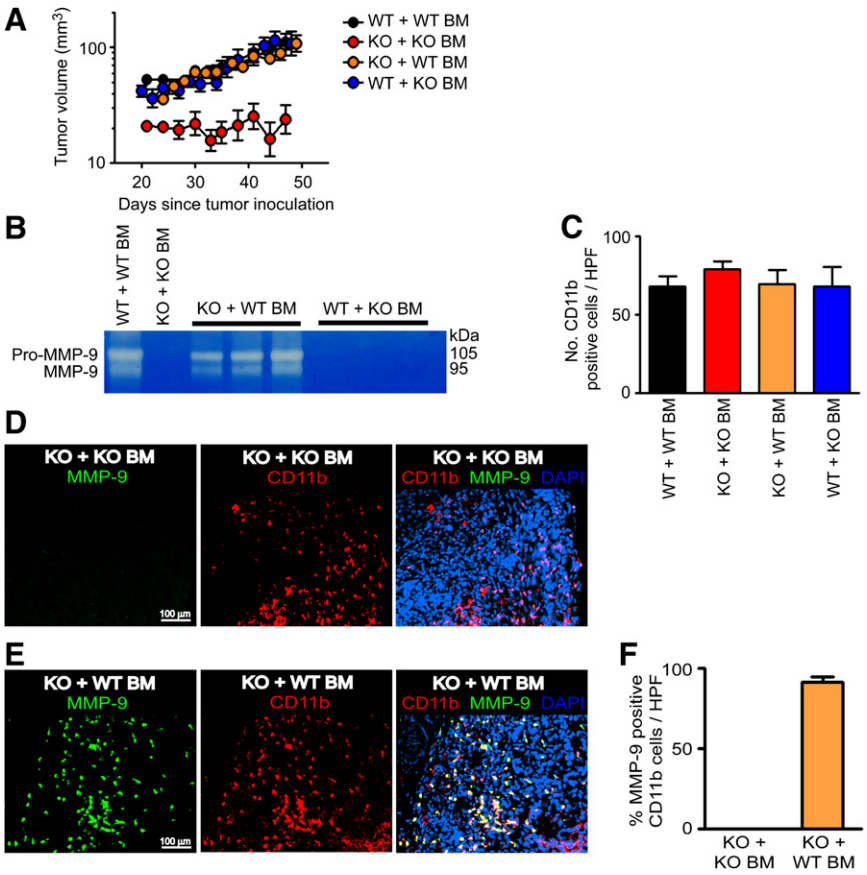

Figure 4. Functional BM Cells Restore Tumor Growth in Preirradiated Tissues of *MMP-9* KO Mice

(A) MT1A2 tumor growth in preirradiated tissues of WT mice that had received the BM cells from WT mice (WT + WT BM), *MMP-9* KO mice receiving BM cells from *MMP-9* KO mice (KO + KO BM), *MMP-9* KO mice receiving BM cells from WT mice (KO + WT BM), or WT mice that had received the BM cells from *MMP-9* KO mice (WT + KO BM). Note that tumor growth was severely impaired in KO + KO BM and was restored in KO + WT BM.

(B) Zymography was used to determine the efficiency of the BM reconstitution. Whole BM cells of the recipients were isolated and analyzed for MMP-9 activity at ≥4 weeks post-BM transplantation. Each lane represents one mouse.

(C) Quantification of CD11b+ myelomonocytic cells in HPF from tumors in (A).

(D) Immunostaining of the tumors from KO + KO BM for CD11b myelomonocytic cells (red) and MMP-9 (green), counterstained with DAPI (blue).

(E) Immunostaining of the tumors from KO + WT BM as in (D).

(F) Quantification of MMP-9- and CD11b-double-positive cells in tumors from KO + KO BM or KO+ WT BM.

Symbols in (A), (C), and (F) are the mean ± SEM for n ≥ 5 mice per group.

in the numbers of CD11b- and MMP-9-double-positive cells (Figure 3B).

In RIF tumors, we similarly observed an increase in MMP-9-positive areas in "IR tumors" and "pre-IR bed," and increased numbers of CD11b- and MMP-9-positive cells in "IR tumors" (Figure 3C). However, we also observed numerous CD11b-negative tumor cells that strongly expressed MMP-9 (Figure 3A and Figure S4A), suggesting that RIF tumor cells themselves are a significant source of MMP-9.

To confirm the histological observations of MMP-9 expression, we performed immunoblots with tumor lysates. We found that IR, either of the tumors directly ("IR tumors") or of the transplantation site ("pre-IR bed"), increased the expression of MMP-9 in both the MT1A2 and RIF tumors (Figure 3D), consistent with the histological observations. The higher expression of MMP-9 in RIF tumors especially from "pre-IR bed" compared to that in MT1A2 tumors is likely due to the strong expression of MMP-9 by the RIF tumor cells.

Genetic Depletion of *MMP-9* Abrogates Tumor Vasculogenesis

To address the role of MMP-9 in vasculogenesis, we used *MMP-9* knockout (KO) mice with tumors grown in preirradiated tissues to inhibit angiogenesis. We selected MT1A2 tumors over RIF tumors because MT1A2 tumors are syngeneic to *MMP-9* KO and wild-type (WT) mice, and the source of MMP-9 in the tumors is largely restricted to CD11b+ myelomonocytic cells, allowing us to investigate the role of the BM-derived CD11b+ myelomonocytic cells in vasculogenesis. We first examined the growth of MT1A2 tumors in *MMP-9* KO and WT mice and found that the tumors grew progressively in the *MMP-9* KO mice, albeit a little slower than in the WT mice (Figure S5A). However, tumor growth in preirradiated tissues was severely impaired in *MMP-9* KO mice (Figure S5B) or in *MMP-9* KO mice that had received BM cells from *MMP-9* KO mice (*MMP-9* KO mice + KO BM) (Figure 4A) compared to their WT counterparts (Figure S5B and Figure 4A).

We next determined whether functional BM could restore tumor growth in preirradiated tissues of *MMP-9* KO mice by transplanting BM cells from WT mice into *MMP-9* KO mice (*MMP-9* KO mice + WT BM). The efficiency of BM reconstitution was confirmed by zymography at the time of tumor implantation (≥4 weeks post-BM transplantation), which showed that the activity of MMP-9 in the BM could be restored in *MMP-9* KO mice or lost in WT mice by transplanting BM cells (Figure 4B). Reconstitution of the BM in *MMP-9* KO mice with WT BM completely restored the growth of the tumors in the preirradiated site to that of WT mice (Figure 4A). However, WT mice receiving BM cells from *MMP-9* KO mice (WT mice + KO BM) showed no difference in tumor growth in preirradiated tissues compared to WT mice + WT BM (Figure 4A), indicating that non-BM-derived cells can compensate for the lack of MMP-9 in BM cells. We examined CD11b+ myelomonocytic cells in the tumors of all four groups and found that there was no significant difference in the number of CD11b+ cells in the tumors from the different groups (Figure 4C). When examined for MMP-9 in tumors grown

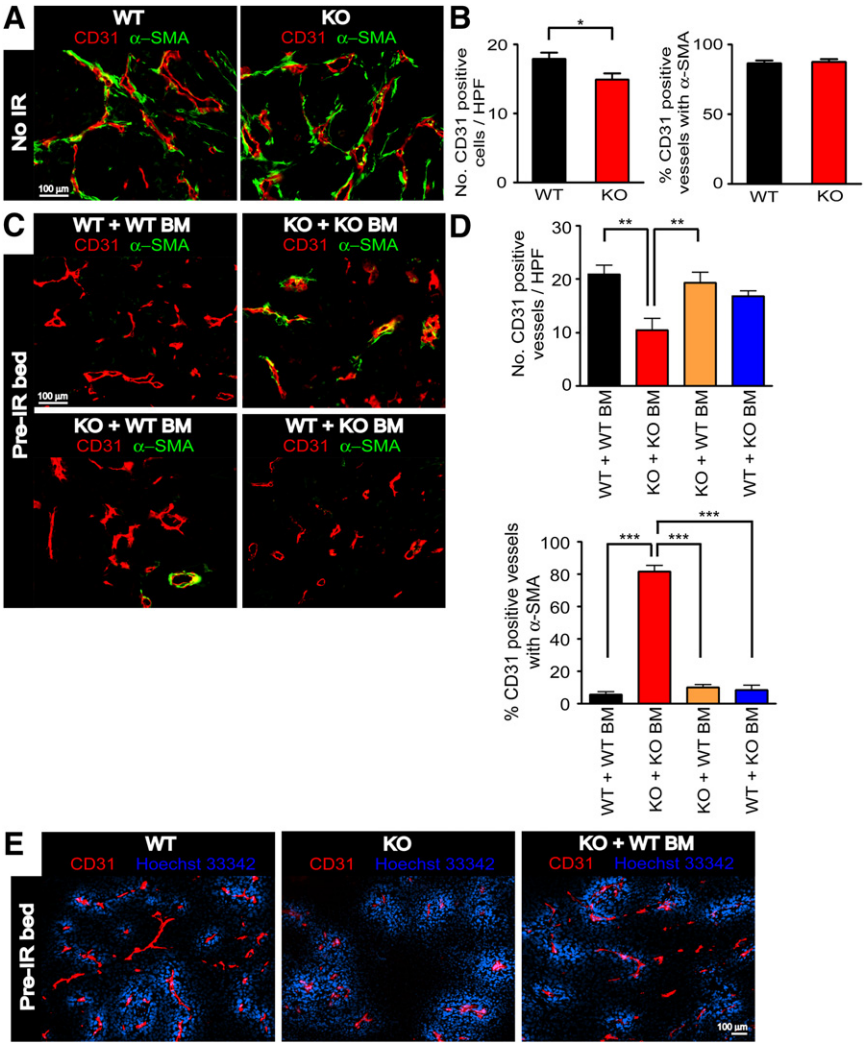

Figure 5. Immature Vessels Are Developed in *MMP-9* KO Mice + WT BM to Support Tumor Growth in Preirradiated Tissues

(A) Immunostaining of CD31 (red) and α-SMA (green) in MT1A2 tumors grown in the wild-type (WT) or *MMP-9* KO (KO) mice.

(B) Number of CD31-positive vessels per HPF (left) and proportions of CD31-positive vessels associated with α-SMA (right) in tumors from (A).

(C) Immunostaining of CD31 (red) and α-SMA (green) for tumors from Figure 4A. Group names are as in Figure 4A.

(D) Quantification of CD31-positive vessels per HPF (upper panel) and proportions of CD31-positive vessels associated with α-SMA (lower panel) in the tumors from (C). Symbols in (B) and (D) are the mean ± SEM for n ≥ 5 animals per group. *p < 0.05, **p < 0.01, and ***p < 0.001, respectively, determined by one-way ANOVA.

(E) Functional blood vessels of tumors grown in preirradiated tissues of WT, KO, or KO + WT BM examined by intravenous infusion with Hoechst 33342 (blue). Tumor sections were stained with CD31 (red).

in preirradiated tissues of *MMP-9* KO mice + WT BM, we found that the majority of MMP-9-positive cells (91% ± 3%) were positive for CD11b (Figures 4E and 4F), while there were no MMP-9-positive CD11b myelomonocytic cells in those tumors from *MMP-9* KO mice + KO BM (Figures 4D and 4F) as expected, or from WT mice + KO BM (Figure 6D). In the tumors from WT mice + KO BM, some MMP-9-positive areas were observed with morphology of smooth muscle- or fibroblast-like cells (Figure S5C). Overall, the results suggest that CD11b+ myelomonocytic cells are the main source of MMP-9 and that these cells can restore tumor growth in irradiated tissues of *MMP-9* KO mice.

To determine whether the restored tumor growth by functional BM was associated with vasculogenesis, we first tested a possibility that CD11b+ myelomonocytic cells differentiate into endothelial cells in tumors. By immunostaining, we observed in tumors of all four groups that CD11b+ cells did not colocalize with CD31 (Figure S5E), suggesting that CD11b+ myelomonocytic cells did not differentiate to the tumor endothelium. This also indicates that CD11b+ myelomonocytic cells indirectly contributed to vasculogenesis. We examined vessel density and maturity in the tumors, determined by the number of CD31-positive vessels and the proportion of CD31-labeled endothelial cells surrounded by pericytes, identified by α-smooth muscle actin (α-SMA) immunostaining. Without IR, most of the vessels in tumors grown in WT (87% ± 2%) or *MMP-9* KO (87% ± 2%) mice were associated with α-SMA (Figures 5A and 5B). In sharp contrast, the vasculature of the tumor growing in the preirradiated site of WT + WT BM was sparsely covered by α-SMA (Figure 5C). This is consistent with our hypothesis of a different etiology of the vessels in the two situations: in the unirradiated tissue most of the vessels arise from angiogenesis (local sprouting), whereas in preirradiated bed they can only arise from vasculogenesis (circulating cells). On the other hand, the majority of the vessels in the very small (and nongrowing) tumors in the irradiated site of *MMP-9* KO mice + KO BM had a mature appearance with extensive α-SMA coverage (Figure 5C). Moreover, while there was little or no difference in the density and maturity of the CD31-positive endothelial cells between the WT and *MMP-9* KO mice without IR (Figure 5B), the vessel density was significantly lower in the very small nongrowing tumors growing in the irradiated site of the *MMP-9* KO mice, and this was restored to WT levels by transplantation of WT BM cells (Figure 5D).

We further examined whether the impaired tumor growth in preirradiated tissues of *MMP-9* KO mice was due to an impairment in the function of the tumor vessels. To investigate this we intravenously injected Hoechst 33342 into WT mice, *MMP-9* KO mice, or *MMP-9* KO mice + WT BM, all of which had tumors implanted in preirradiated tissues. We found that the vessels were well-perfused in the tumors grown in preirradiated tissues of *MMP-9* KO mice and that there was no difference in functionality of vessels in the tumors between WT mice, *MMP-9* KO mice, or *MMP-9* KO mice + WT BM (Figure 5E).

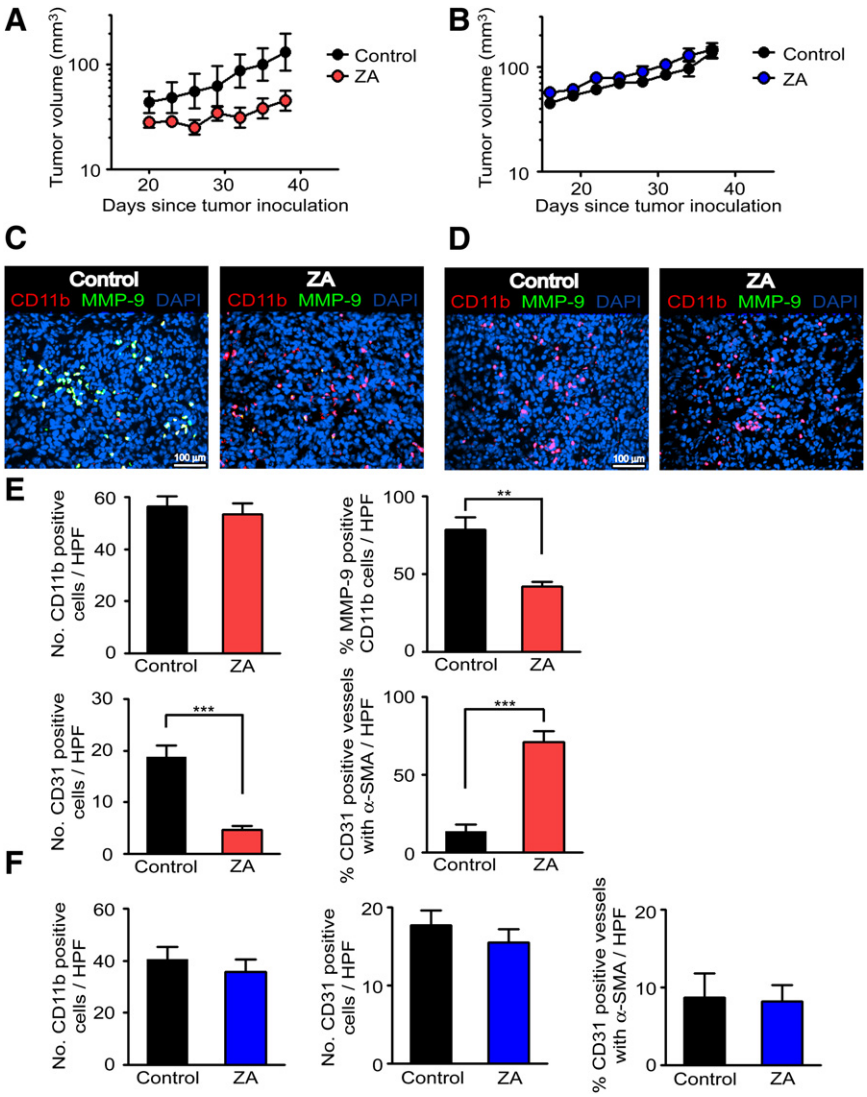

Figure 6. Pharmacological Targeting of MMP-9 in CD11b+ Myelomonocytic Cells by ZA Inhibits Tumor Growth in the Preirradiated Site

(A) MT1A2 tumor growth with (ZA, n = 5) or without (control, n = 4) ZA in preirradiated tissues of *MMP-9* KO mice that had received BM cells from WT mice.

(B) MT1A2 tumor growth in preirradiated tissues of WT mice receiving BM cells from *MMP-9* KO mice. n = 5 animals per group. Symbols and error bars in (A) and (B) are the mean ± SEM.

(C) Immunostaining of the tumors from (A) for MMP-9 (green), CD11b (red), and nuclei (blue).

(D) Immunostaining of the tumors from (B) as in (C).

(E) Quantification of CD11b+ cells (upper left), percentage of MMP-9-expressing CD11b+ cells (upper right), CD31-positive endothelial cells (lower left), and CD31-positive vessels that were associated with α-SMA (lower right) in the tumors from (A).

(F) Quantification of the parameters as in (E) but from tumors in (B).

Error bars in (E) and (F) are SEM. **p < 0.01 and ***p < 0.001, respectively, determined by two-tailed Student's t test.

Taken together, these data suggest that the failure of the tumors to grow in the preirradiated site of *MMP-9* KO mice was the result of abrogation of both angiogenesis (by irradiation) and of vasculogenesis (by lack of MMP-9 in BM-derived cells), and that the blood vessels within the tumors (Figure 5) and around the periphery (Figure S5D) of the small tumors in the preirradiated tissue of *MMP-9* KO mice were mature and well-perfused normal vessels, probably co-opted by growth of the tumor into surrounding normal tissue. Overall, it suggests that restoration of tumor growth in the irradiated tissue by WT BM allowed immature vessels to form by MMP-9 expressing CD11b+ myelomonocytic cells that arose from the transplanted BM.

Pharmacological Inhibition of CD11b+ Myelomonocytic Cells Expressing MMP-9 Significantly Reduces Tumor Growth in Preirradiated Tissues

Based on the above results, we hypothesized that selective inhibition of CD11b+ myelomonocytic cells expressing MMP-9 would inhibit BM-derived vasculogenesis and tumor growth in preirradiated tissues. To test this, we used the aminobisphosphonate zolendronic acid (ZA, Zometa), a clinically available agent to ameliorate bone metastases that was recently reported to selectively target MMP-9 expressing macrophages in K14-HPV16 cervical carcinoma in mice (Giraudo et al., 2004). MT1A2 tumors were grown in the preirradiated tissues in *MMP-9* KO mice that had received BM cells from WT mice (*MMP-9* KO mice + WT BM) as previously described. Hence tumors grown in these mice, the major source of MMP-9, would come from the BM-derived CD11b+ myelomonocytic cells. In order to determine the specific activity of ZA in targeting MMP-9 from BM-derived cells but not from other tissues, we also tested ZA in WT mice receiving BM cells from *MMP-9* KO mice (WT mice + KO BM). Because WT mice + KO BM do not have MMP-9 expressing CD11b+ myelomonocytic cells, the tumor growth in preirradiated tissues of these mice should not be affected by the ZA treatment. Treatment with ZA at 100 μg/kg intraperitoneally once per day for up to 6 weeks produced a significant inhibition of tumor growth in the irradiated site of *MMP-9* KO mice + WT BM (Figure 6A). In contrast, there was no effect of ZA on tumor growth of WT mice + KO BM (Figure 6B), as predicted. Histological examinations showed that ZA-treated tumors in *MMP-9* KO mice + WT BM had similar numbers of CD11b+ myelomonocytic cells but a smaller fraction that were MMP-9 positive (Figures 6C and 6E). In addition, ZA-treated tumors showed significantly fewer numbers of CD31-positive vessels than the control tumors (Figure 6E). When examined for vessel maturity, ZA-treated tumors had significantly more vessels associated with α-SMA than the control tumors (Figure 6E), in agreement with the data obtained with *MMP-9* KO mice + KO BM

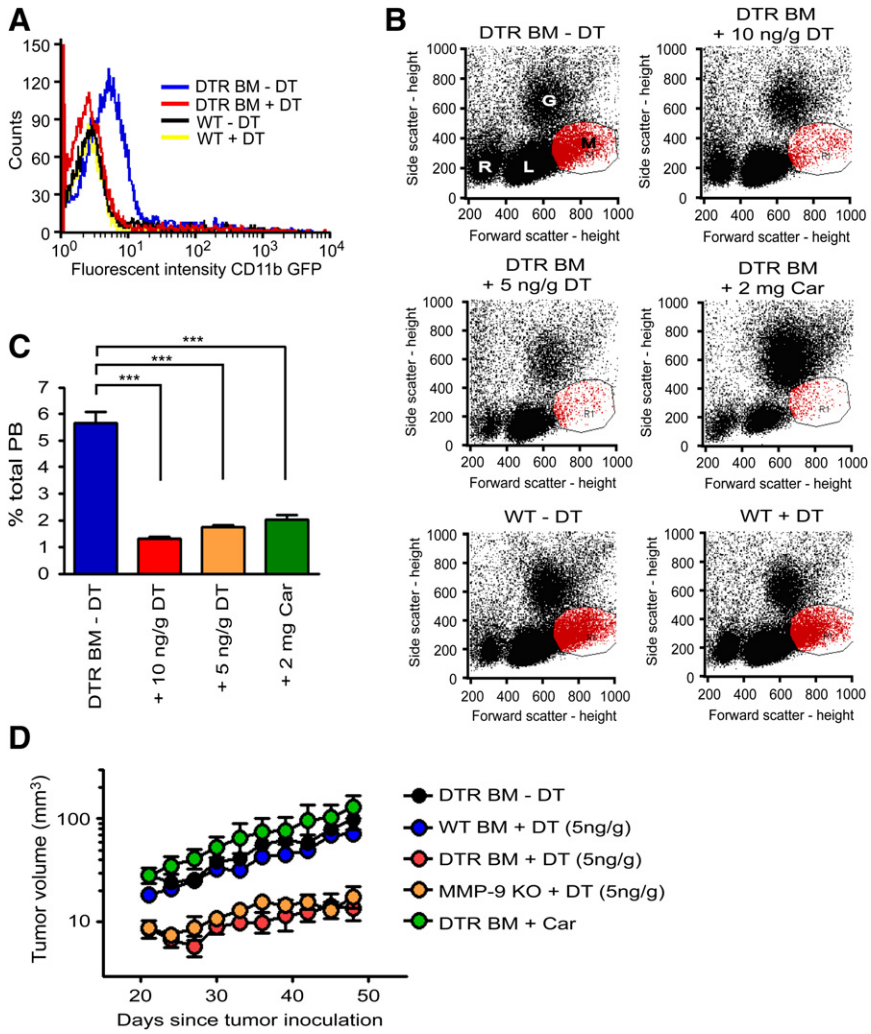

Figure 7. Depletion of CD11b+ Cells Expressing MMP-9 by DT Further Abrogates Tumor Growth in Preirradiated Tissues of *MMP-9* KO + DTR BM

(A) Peripheral blood of *MMP-9* KO mice that had received BM cells from transgenic mice expressing diphtheria toxin receptor (DTR) and GFP driven by CD11b promoter (DTR BM) or of WT mice without BM transplantation (WT). These mice were treated with or without diphtheria toxin (DT, 10 ng/g). Blood was analyzed for GFP fluorescent intensity as an indicator of CD11b levels at 24 hr posttreatment. Note that treatment with DT 10 ng/g in DTR BM mice resulted in GFP signal similar to that in WT mice with or without DT.

(B) Peripheral blood of *MMP-9* KO mice + DTR BM (DTR BM) treated without DT (-DT), with 10 ng/g DT, 5 ng/g DT, or 2 mg/g carrageenan (Car) at 24 hr posttreatment. Blood of WT mice (WT) with and without DT 10 ng/g is also shown. R, red blood cells; L, lymphocytes; G, granulocytes; M, monocytes.

(C) Quantification of monocytes gated in red from (B). Symbols and error bars indicate the mean ± SEM for $n \geq 5$ mice per group. ***$p < 0.001$ analyzed by one-way ANOVA.

(D) MT1A2 tumor growth in preirradiated tissues of *MMP-9* KO mice + DTR BM (DTR BM) without DT (−DT, n = 4), with DT (5 ng/g, n = 5), or with Car (n = 4). Tumors were also grown in preirradiated tissues of WT mice receiving BM cells from WT mice (WT BM, n = 5) or *MMP-9* KO mice (*MMP-9* KO, n = 5) that were treated with DT (5 ng/g). Error bars indicate SEM.

(Figure 5). In WT mice + KO BM, we did not observe any CD11b+ myelomonocytic cells that were MMP-9 positive (Figure 6D), and there was no significant difference in the number of CD11b+ cells between ZA-treated and control tumors (Figure 6F). As found earlier, the percentage of CD31-positive tumor vessels and those associated with α-SMA was low in the WT mice + KO BM, and this was not affected by ZA (Figure 6F). In summary, ZA efficiently targeted MMP-9 expressed in the BM-derived CD11b+ myelomonocytic cells in the tumor, inhibited the growth of tumors in the preirradiated tissues, and reduced the numbers of immature (tumor-like) vessels in the tumors.

Conditional Ablation of CD11b+ Myelomonocytic Cells Further Abrogates Tumor Growth in Preirradiated Tissues of *MMP-9* KO Mice + Functional BM Cells

We further examined the role of CD11b+ myelomonocytic cells in restoring tumor growth in preirradiated tissues by conditionally ablating CD11b+ cells. To do this, we transplanted BM cells from transgenic mice expressing human diphtheria toxin receptor (DTR) and GFP driven by the *CD11b* promoter (Stoneman et al., 2007) into lethally irradiated *MMP-9* KO mice (*MMP-9* KO mice + DTR BM). Treatment by diphtheria toxin (DT, 10 ng/g) of *MMP-9* KO mice + DTR BM effectively depleted GFP-positive CD11b+ cells in the peripheral blood at 24 hr postadministration (Figure 7). In contrast, administration of DT in WT mice showed no depletion of CD11b+ myelomonocytic cells (Figures 7A and 7B). However, repeated administration of DT 10 ng/g once in every 2 days in *MMP-9* KO mice + DTR BM resulted in mortality in 20 days (Figure S6A). We therefore lowered the dose of DT to 5 ng/g once every 2 days and still observed effective depletion of CD11b+ myelomonocytic populations in the peripheral blood of *MMP-9* KO mice + DTR BM (Figures 7B and 7C). The depleted CD11b+ cells rebounded to untreated levels at 48 hr (data not shown). We also tested another approach to deplete CD11b+ cells by using carrageenan, a compound that eliminates macrophages (Li et al., 2007). Although carrageenan at 2 mg/mouse showed effective depletion of CD11b+ myelomonocytic cells at 24 hr (Figures 7B and 7C), it also resulted in a significant expansion of granulocyte populations (Figure 7B). Moreover, carrageenan-treated mice showed significant bodyweight loss and some early mortality (Figures S6A and S6B). The dose of carrageenan was therefore lowered to 1 mg/mouse, but once per week treatment was ineffective in maintaining low levels of CD11b+ myelomonocytic cells (data not shown).

When tumors were implanted in preirradiated tissues of these mice, tumor growth was significantly inhibited in *MMP-9* KO mice + DTR BM receiving DT (5 ng/g), mimicking the lack of tumor growth in *MMP-9* KO mice (Figure 7D). Treatment with DT in WT mice + WT BM showed no effect in tumor growth (Figure S6E). Carrageenan, on the other hand, did not inhibit tumor growth (Figure 7D), likely due to the rebound of CD11b+ myelomonocytic cells resulting from the once a week treatment regimen. Overall, these results further demonstrate that MMP-9 expressing CD11b+ myelomonocytic cells play an essential role in promoting tumor growth in preirradiated tissues.

DISCUSSION

In this study, we show the crucial role played by the ECM degrading enzyme MMP-9 provided by BM-derived CD11b+ myelomonocytic cells in allowing tumors to grow in irradiated normal tissues of the mice. We used the irradiated tumor bed model to abrogate local angiogenesis so as to examine the role of BM-derived cells in tumor growth. We demonstrate that CD11b+ myelomonocytic cells are recruited into irradiated tumors and into tumors growing in preirradiated tissues, and these cells restored tumor growth in *MMP-9* KO mice by allowing immature blood vessels to develop. Further, when MMP-9 or a major source of MMP-9-expressing cells are genetically absent, ablated, or chemically inhibited, tumors in preirradiated tissues fail to grow beyond a very small size and are composed of normal, mature blood vessels.

Given the role of MMP-9 in degrading and remodeling the ECM, CD11b+ myelomonocytic cells expressing MMP-9 are likely to be important in reorganizing stromal compartments of tumors. In particular, by degrading the ECM they could provide a means for endothelial cells to enter or migrate to the tumor when the existing endothelial cells in and adjacent to the tumor cannot proliferate because of the local irradiation they have received. MMP-9 is involved in cleaving fibrillar type I collagen, the major constituent of the extracellular matrix to which endothelial cells are exposed in an injured tissue, allowing growth factor-induced angiogenesis to occur (Seandel et al., 2001). Moreover, MMP-9 provided by BM-derived macrophages has been shown to be essential in capillary branching in ischemia-induced revascularization of normal tissues (Johnson et al., 2004). MMP-9 may also enhance local angiogenesis in a spatiotemporal manner due to its ability to cleave membrane-bound VEGF, thereby increasing bioavailable levels of VEGF (Bergers et al., 2000), a growth factor that is critical for survival and growth of endothelial cells (Ferrara et al., 2003). Macrophages themselves can also express VEGF, and these cells are observed in poorly vascularized areas of human breast carcinoma (Lewis et al., 2000). Other functions of macrophages, such as inducible nitric oxide synthase, arginase, and cyclooxygenase-2, have been reported to be important in growth of irradiated tumors in mice (Tsai et al., 2007).

CD11b+ myelomonocytic cells, including a subset of $CD11b^{+}Gr\text{-}1^{+}$ myeloid suppressor cells, are increasingly recognized for their roles in promoting tumor progression. Studies have shown that these cells enhance tumor angiogenesis (Yang et al., 2004), prepare the premetastatic niche in the lung (Hiratsuka et al., 2006), and are responsible for the refractoriness of tumors to anti-VEGF treatment (Shojaei et al., 2007). Our study is consistent with these reports by showing that they promote tumor growth in preirradiated tissues of mice when local angiogenesis is inhibited.

Increased leukocyte infiltration, especially by CD68-positive macrophages, is observed in biopsy samples of rectal cancer patients after high-dose (and short-term) and low-dose (and long-term) fractionated radiotherapy (Baeten et al., 2006). The authors of this study proposed that an increased expression of adhesion molecules such as intracellular adhesion molecule-1, vascular cell adhesion molecule, and E-selectin on tumor endothelium after radiotherapy is responsible for stimulating leukocyte infiltration in the tumors. However, other factors, including VEGF and stromal-cell derived factor-1 (SDF-1), have been also reported to be essential in recruiting BM-derived myelomonocytic cells to tumors (Grunewald et al., 2006; Petit et al., 2007). VEGF and SDF-1 are downstream targets of hypoxia-inducible factor-1 (HIF-1), a transcription factor induced by hypoxia due to stabilization under hypoxic conditions (Ceradini et al., 2004; Semenza, 2003). HIF-1 levels are likely to increase in tumors regrowing after irradiation or tumors grown in preirradiated tissues due to the increased levels of hypoxia (Kim et al., 1993; Teicher et al., 1994). Furthermore, recent studies have shown that irradiation increases HIF-1 activity in tumors (Moeller et al., 2004), and this occurs by recruited macrophages in irradiated tumors producing nitric oxide, which in turn nitrosylates cysteine residues of the oxygen-dependent degradation domain of HIF-1α, thereby stabilizing it (Li et al., 2007).

Overall, there is strong evidence that BM-derived myelomonocytic cells promote tumor growth and that they do so by forming a positive feedback loop with many other components of the tumor microenvironment. Indeed, several investigators have reported that targeting TAMs produces significant antitumor activity (Allavena et al., 2005; Lin et al., 2001; Luo et al., 2006; Zeisberger et al., 2006). However, it is evident that tumors show large variations in recruiting and utilizing these BM-derived cells, and our study demonstrates that the pattern of BM-derived infiltrates and reliance for the source of MMP-9 varies widely between RIF and MT1A2 tumors. Hence, prospective knowledge of tumor cytokines and their role in the recruitment of BM-derived cells will be important to derive maximum antitumor activity from therapies targeting these cells.

We observed a minimal contribution of BM-derived EPCs to the vasculature of tumors grown in preirradiated tissues. This raises the question as to the source of the additional endothelial cells. Studies have shown that there are mature circulating endothelial cells derived from vessel wall turnover and that these cells are increased in patients with some types of cancer (Bertolini et al., 2006). Recently, Aicher and colleagues reported that there are non-BM-derived circulating progenitor cells from organs such as the small intestine and liver and that these cells incorporate into sites of neovascularization (Aicher et al., 2007). However, further studies are needed to determine the exact source of those new endothelial cells that promote tumor growth following high-dose radiotherapy.

Our results also suggest that BM-derived cells expressing MMP-9 are sufficient but not essential for tumor vasculogenesis. This is evident from the similar tumor growth in preirradiated tissues of WT mice + *MMP-9* KO BM compared to WT mice + WT

BM. These data indicate that non-BM cells of the host that are still proficient in MMP-9, such as fibroblasts and smooth muscle cells, can compensate for the deficiency of MMP-9 from BM cells. MMP-9 in fibroblasts has been shown to promote mitogenic induction of breast cancer cells by enhancing endothelial cell survival and function in an in vitro coculture model (Shekhar et al., 2001). This supports our observation that other sources of MMP-9 could also play a role in promoting tumor growth and angiogenesis. It also strengthens the rationale that MMP-9 is an important target for adjunct therapy to radiotherapy.

Clinical trials with MMP inhibitors have been uniformly disappointing. Although MMP-9 expression has been shown to correlate with tumor response in patients (Unsal et al., 2007), MMP inhibitors when given alone or in combination with cytotoxic agents showed no gain in clinical efficacy (Coussens et al., 2002). However, none of these trials have been performed in conjunction with radiotherapy, a therapy that can selectively inhibit local angiogenesis and make tumor growth dependent on vasculogenesis. Even though currently available MMP-9 inhibitors lack specificity for MMP-9 by also inhibiting the closely related MMP-2, a recent preclinical study showed that the MMP-2 and MMP-9 inhibitor Metastat significantly potentiated the antitumor efficacy of irradiation (Kaliski et al., 2005), supporting the rationale of combining MMP inhibitors with radiotherapy. We believe that our data point the way to further studies of MMP-9 inhibitors with radiation.

EXPERIMENTAL PROCEDURES

Mice

All animal procedures were approved by Stanford's Administrative Panel on Laboratory Animal Care (APLAC). All mice except C3H [FVB/N-TgN(*TIE2*-lacZ)182Sato; B6.Cg-Tg(*TIE2*GFP)287Sato/1J; B6;129S-Gt(ROSA)26Sor/J; FVB-Tg(ITGAM-DTR/EGFP)34Lan/J; FVB.Cg-Tg(GFPU)5Nagy/J; FVB.Cg-*Mmp9*^{tm1Tvu}/J; FVB/NJ; and C57Bl/6J] were purchased from the Jackson laboratory (Bar Harbor, ME). C3H mice were obtained from the breeding facility at Stanford University's Research Animal Facility. Mice were maintained in a germ-free environment and had access to food and water available ad libitum.

Bone Marrow Transplantation

Six- to twelve-week-old mice were used as BM recipients and donors. BM cells from the donors were harvested from both femurs and tibias by flushing the bone cavity with Hank's balanced salt solution (Invitrogen, Carlsbad, CA) using 25 gauge needles (BD, Franklin Lakes, NJ). The recipient mice were lethally irradiated 24 hr prior to the BM transplantation. The IR doses used were 9 Gy for FVB, *MMP-9* KO, and C3H mice, and 9.5 Gy for C57Bl/6 mice. The lethally irradiated mice received >2 × 10^6 BM cell suspensions intravenously and were allowed to recover for a minimum of 4 weeks.

Cell Lines

The MT1A2 mouse mammary carcinoma cell line was obtained from Dr. Frank Graham (McMaster University, Canada), the TG1-1 mouse mammary carcinoma cell line was from Dr. Rakish Jain (Harvard University, MA), the 6780 lymphoma cell line was from Dr. Dean Felsher (Stanford University, CA), and the B16F1 melanoma cell line was from Dr. Garth Nicolson (UC Irvine, CA). The LLC cell line was purchased from the American Tissue Culture Collection (Manassas, VA). MT1A2, TG1-1, RIF, B16F1, and LLC cells were maintained in Dulbecco's modified Eagle's medium (Invitrogen, Carlsbad, CA) supplemented with 10% fetal bovine serum (FBS; Mediatech, Inc., Herndon, VA), and penicillin-streptomycin (1%). 6780 cells were grown in RPMI (Invitrogen) supplemented with 10% FBS, and penicillin-streptomycin (1%). RIF cells were constantly passaged in vitro-in vivo by implanting in syngeneic female C3H mice as described previously (Twentyman et al., 1980).

Tumor Implantation, Irradiation, Measurement, and Perfusion

The MT1A2 and TG1-1 cells were inoculated at 1.5 × 10^6 cells/mouse, 6780 cells at 5 × 10^6 cells/mouse, and RIF, B16F1, or LLC cells at 5 × 10^5 cells/mouse intradermally on the back of the mouse approximately 1 cm proximal to the base of the tail. Unanesthetized mice were placed in lead jigs through which the tumor implantation site or established tumors (at approximately 200 mm^3 in volume) were protruded for irradiation to an area of approximately 2 cm diameter. Irradiation was performed with a Phillips X-ray unit operated at 200 kVp with the dose rate of 1.21 Gy/min (20 mÅ with added filtration of 0.5 mm copper, the distance from X-ray source to the target of 31 cm, and a half value layer of 1.3 mm copper). For the tumors grown in the preirradiated site, the tumors were implanted 5 days after irradiation. Tumor volume (V) was calculated using the formula for a spheroid: $V = \pi/6 \times (\text{width})^2 \times (\text{length})$. When tumor volumes reached approximately 200 mm^3 for control tumors and slightly more than 200 mm^3 for irradiated tumors and tumors grown in the irradiated bed, cardiac perfusion was performed in asphyxiated tumor-bearing mice with 4% paraformaldehyde in phosphate-buffered saline (PBS; Invitrogen). Tumors were removed, embedded in optimal cutting temperature (OCT) compound (Sakura Finetek, Torrance, CA), and frozen in −80°C until cryosectioning and immunostaining.

Immunostaining

Primary antibodies for immunofluorescent staining were a rat monoclonal CD31/PECAM-1 (MEC13.3; BD PharMingen, San Diego, CA), a rabbit polyclonal GFP antibody (Invitrogen, Eugene, OR), a rabbit polyclonal MMP-9 (Abcam, Cambridge, MA), a biotinylated CD11b/macrophage-associated antigen-1α (M1/70; BD PharMingen), a biotinylated CD11c (HL3; BD PharMingen), and a biotinylated Gr-1/Ly-6C (RB6-8C5; BD PharMingen). Primary antibodies were detected by using secondary antibodies of anti-rat Alexa Fluor 594 (Invitrogen), anti-rabbit Alexa Fluor 488 (Invitrogen), anti-rabbit Alexa Fluor 647 (Invitrogen), or streptavidin Alexa Fluor 555 (Invitrogen). FITC-conjugated anti-mouse α-smooth muscle actin (α-SMA) antibody (Sigma, St. Louis, MO) was used to detect pericytes, and Phycoerythrin (PE)-conjugated antibodies for CD4 (StemCell Technologies, Vancouver, BC, Canada), CD8α/Ly-2 (53-6.7; BD PharMingen), and CD49b (StemCell Technologies) were used to detect CD4, CD8α T cells, and NK cells, respectively. Frozen sections of tumors (8 μm) were dried in air, hydrated with PBS, blocked with 5% goat serum in PBS (containing 0.03% Triton X-100) for 30 min, and incubated with primary antibodies for 2 hr at room temperature (RT). Sections were washed three times in PBS, followed by secondary antibody for 1 hr at RT. After washing in PBS, sections were mounted with anti-fade reagent with 4′,6-diamidino-2-phenylindole (DAPI) (Invitrogen) and viewed with a Leica DMRA2 microscope (Wetzlar, Germany) using PLAN 20×/0.40 and 40×/0.65 objective lenses with HC PLAN s 10×/22 eyepieces. Images were acquired with a Hamamatsu ORCA-ER camera and Improvision OpenLab software.

Histological Assessment

MMP-9-positive area in the tumors was determined by the point-count method (Gray, 1996). Briefly, the proportions were calculated as the number of points directly over MMP-9-positive staining divided by the total number of points examined using a six-point grid in a 15× eyepieces at a 10× objective.

Quantitative analysis for CD11b- and MMP-9-positive cells was done by counting the number of cells in the photographed fields where the most CD11b were observed in nonnecrotic regions using a 40× objective with 10× eyepieces of the DMRA2 fluorescent microscope. X-gal-positive cells were counted in five random fields per tumor with a 20× objective and 10× eyepieces of the DMLB microscope. Quantification was made on three to five independent specimens per tumor, four to five animals per group.

Drug Treatment

ZA (Zometa; Novartis Pharma AG) was dissolved in sterile water and stored long term at −80°C and at 4°C for short-term storage as reported previously (Giraudo et al., 2004). Mice were treated every day with ZA or water from the first day of the local irradiation at the lower back. The animals were monitored during the treatment for their bodyweight to assess side effects and did not show any significant loss in weight (less than 10% of bodyweight).

DT (List biological laboratories Inc., CA) was prepared in sterile water containing 1% of bovine serum albumin (BSA, Sigma). Carrageenan (Sigma) was dissolved in saline at 10 mg/ml. Mice were treated with DT or vehicle (1% BSA in water) once in 2 days or carrageenan once per week by intraperitoneal injections from the first day of the local irradiation. The treated animals received water containing antibiotics (neomycin and polymyxin B) throughout the study.

Statistical Analysis

Statistical comparisons of data sets were performed by a two-tailed Student's t test or one-way ANOVA with Tukey post test (V4.00 GraphPad Inc., CA). The data were considered to be significantly different when $p < 0.05$.

SUPPLEMENTAL DATA

The Supplemental Data include Supplemental Experimental Procedures and six supplemental figures and can be found with this article online at http://www.cancercell.org/cgi/content/full/13/3/193/DC1/.

ACKNOWLEDGMENTS

We would like to thank Dr. Frank Graham (McMaster University, Canada) for providing the MT1A2 mouse mammary carcinoma cell line, Dr. Rakish Jain (Harvard University) for the TG1-1 mouse mammary carcinoma cell line, Dr. Dean Felsher (Stanford University) for the 6780 lymphoma cell line, Dr. Mary Jo Dorie for culturing RIF cells, Mr. Doug Menke for intravenous injection of BM cells, and Ms. Pauline Chu for frozen sections and H&E staining. Support was provided by the Stanford University Ludwig Translational Program in Cancer Research, a Translational Cancer Research Award from the Stanford Comprehensive Cancer Center, and the National Institutes of Health grant RO1 CA-118202.

Received: May 4, 2007
Revised: October 16, 2007
Accepted: November 28, 2007
Published: March 10, 2008

REFERENCES

Aicher, A., Rentsch, M., Sasaki, K., Ellwart, J.W., Fandrich, F., Siebert, R., Cooke, J.P., Dimmeler, S., and Heeschen, C. (2007). Nonbone marrow-derived circulating progenitor cells contribute to postnatal neovascularization following tissue ischemia. Circ. Res. *100*, 581–589.

Allavena, P., Signorelli, M., Chieppa, M., Erba, E., Bianchi, G., Marchesi, F., Olimpio, C.O., Bonardi, C., Garbi, A., Lissoni, A., et al. (2005). Anti-inflammatory properties of the novel antitumor agent yondelis (trabectedin): Inhibition of macrophage differentiation and cytokine production. Cancer Res. *65*, 2964–2971.

Baeten, C.I.M., Castermans, K., Lammering, G., Hillen, F., Wouters, B.G., Hillen, H.F.P., Griffioen, A.W., and Baeten, C.G.M. (2006). Effects of radiotherapy and chemotherapy on angiogenesis and leukocyte infiltration in rectal cancer. Int. J. Radiat. Oncol. Biol. Phys. *66*, 1219–1227.

Bailey, A.S., Willenbring, H., Jiang, S., Anderson, D.A., Schroeder, D.A., Wong, M.H., Grompe, M., and Fleming, W.H. (2006). Myeloid lineage progenitors give rise to vascular endothelium. Proc. Natl. Acad. Sci. USA *103*, 13156–13161.

Bergers, G., and Coussens, L.M. (2000). Extrinsic regulators of epithelial tumor progression: Metalloproteinases. Curr. Opin. Genet. Dev. *10*, 120–127.

Bergers, G., Brekken, R., McMahon, G., Vu, T.H., Itoh, T., Tamaki, K., Tanzawa, K., Thorpe, P., Itohara, S., Werb, Z., and Hanahan, D. (2000). Matrix metalloproteinase-9 triggers the angiogenic switch during carcinogenesis. Nat. Cell Biol. *2*, 737–744.

Bertolini, F., Shaked, Y., Mancuso, P., and Kerbel, R.S. (2006). The multifaceted circulating endothelial cell in cancer: Towards marker and target identification. Nat. Rev. Cancer *6*, 835–845.

Capoccia, B.J., Shepherd, R.M., and Link, D.C. (2006). G-CSF and AMD3100 mobilize monocytes into the blood that stimulate angiogenesis in vivo through a paracrine mechanism. Blood *108*, 2438–2445.

Ceradini, D.J., Kulkarni, A.R., Callaghan, M.J., Tepper, O.M., Bastidas, N., Kleinman, M.E., Capla, J.M., Galiano, R.D., Levine, J.P., and Gurtner, G.C. (2004). Progenitor cell trafficking is regulated by hypoxic gradients through HIF-induction of SDF-1. Nat. Med. *10*, 858–864.

Coussens, L.M., Tinkle, C.L., Hanahan, D., and Werb, Z. (2000). MMP-9 supplied by bone marrow-derived cells contributes to skin carcinogenesis. Cell *103*, 481–490.

Coussens, L.M., Fingleton, B., and Matrisian, L.M. (2002). Matrix metalloproteinase inhibitors and cancer: Trials and tribulations. Science *295*, 2387–2392.

De Palma, M., Venneri, M.A., Roca, C., and Naldini, L. (2003). Targeting exogenous genes to tumor angiogenesis by transplantation of genetically modified hematopoietic stem cells. Nat. Med. *9*, 789–795.

Dirkx, A.E., Oude Egbrink, M.G., Wagstaff, J., and Griffioen, A.W. (2006). Monocyte/macrophage infiltration in tumors: Modulators of angiogenesis. J. Leukoc. Biol. *80*, 1183–1196.

Ferrara, N., Gerber, H.P., and LeCouter, J. (2003). The biology of VEGF and its receptors. Nat. Med. *9*, 669–676.

Fujiyama, S., Amano, K., Uehira, K., Yoshida, M., Nishiwaki, Y., Nozawa, Y., Jin, D., Takai, S., Miyazaki, M., Egashira, K., et al. (2003). Bone marrow monocyte lineage cells adhere on injured endothelium in a monocyte chemoattractant protein-1-dependent manner and accelerate reendothelialization as endothelial progenitor cells. Circ. Res. *93*, 980–989.

Galis, Z.S., and Khatri, J.J. (2002). Matrix metalloproteinases in vascular remodeling and atherogenesis: The good, the bad, and the ugly. Circ. Res. *90*, 251–262.

Gill, M., Dias, S., Hattori, K., Rivera, M.L., Hicklin, D., Witte, L., Girardi, L., Yurt, R., Himel, H., and Rafii, S. (2001). Vascular trauma induces rapid but transient mobilization of VEGFR2(+)AC133(+) endothelial precursor cells. Circ. Res. *88*, 167–174.

Giraudo, E., Inoue, M., and Hanahan, D. (2004). An amino-bisphosphonate targets MMP-9-expressing macrophages and angiogenesis to impair cervical carcinogenesis. J. Clin. Invest. *114*, 623–633.

Gothert, J.R., Gustin, S.E., van Eekelen, J.A., Schmidt, U., Hall, M.A., Jane, S.M., Green, A.R., Gottgens, B., Izon, D.J., and Begley, C.G. (2004). Genetically tagging endothelial cells in vivo: Bone marrow-derived cells do not contribute to tumor endothelium. Blood *104*, 1769–1777.

Gray, T. (1996). Quantitation in histopathology. In Theory and Practice of Histological Techniques, J.D. Bancroft and M. Gamble, eds. (New York: Churchill-Livingstone), pp. 641–663.

Grunewald, M., Avraham, I., Dor, Y., Bachar-Lustig, E., Itin, A., Jung, S., Chimenti, S., Landsman, L., Abramovitch, R., and Keshet, E. (2006). VEGF-induced adult neovascularization: Recruitment, retention, and role of accessory cells. Cell *124*, 175–189.

Guy, C.T., Cardiff, R.D., and Muller, W.J. (1992). Induction of mammary tumors by expression of polyomavirus middle T oncogene: A transgenic mouse model for metastatic disease. Mol. Cell. Biol. *12*, 954–961.

Heissig, B., Hattori, K., Dias, S., Friedrich, M., Ferris, B., Hackett, N.R., Crystal, R.G., Besmer, P., Lyden, D., Moore, M.A., et al. (2002). Recruitment of stem and progenitor cells from the bone marrow niche requires MMP-9 mediated release of kit-ligand. Cell *109*, 625–637.

Heissig, B., Hattori, K., Friedrich, M., Rafii, S., and Werb, Z. (2003). Angiogenesis: Vascular remodeling of the extracellular matrix involves metalloproteinases. Curr. Opin. Hematol. *10*, 136–141.

Hiratsuka, S., Watanabe, A., Aburatani, H., and Maru, Y. (2006). Tumour-mediated upregulation of chemoattractants and recruitment of myeloid cells predetermines lung metastasis. Nat. Cell Biol. *8*, 1369–1375.

Itasaka, S., Komaki, R., Herbst, R.S., Shibuya, K., Shintani, T., Hunter, N.R., Onn, A., Bucana, C.D., Milas, L., Ang, K.K., and O'Reilly, M.S. (2007). Endostatin improves radioresponse and blocks tumor revascularization after radiation

therapy for A431 xenografts in mice. Int. J. Radiat. Oncol. Biol. Phys. *67*, 870–878.

Jodele, S., Chantrain, C.F., Blavier, L., Lutzko, C., Crooks, G.M., Shimada, H., Coussens, L.M., and DeClerck, Y.A. (2005). The contribution of bone marrow-derived cells to the tumor vasculature in neuroblastoma is matrix metalloproteinase-9 dependent. Cancer Res. *65*, 3200–3208.

Johnson, C., Sung, H.-J., Lessner, S.M., Fini, M.E., and Galis, Z.S. (2004). Matrix metalloproteinase-9 is required for adequate angiogenic revascularization of ischemic tissues. Potential role in capillary branching. Circ. Res. *94*, 262–268.

Kaliski, A., Maggiorella, L., Cengel, K.A., Mathe, D., Rouffiac, V., Opolon, P., Lassau, N., Bourhis, J., and Deutsch, E. (2005). Angiogenesis and tumor growth inhibition by a matrix metalloproteinase inhibitor targeting radiation-induced invasion. Mol. Cancer Ther. *4*, 1717–1728.

Kim, I.H., Lemmon, M.J., and Brown, J.M. (1993). The influence of irradiation of the tumor bed on tumor hypoxia: Measurements by radiation response, oxygenation electrodes, and nitroimidazole binding. Radiat. Res. *135*, 411–417.

Lewis, C.E., and Pollard, J.W. (2006). Distinct role of macrophages in different tumor microenvironments. Cancer Res. *66*, 605–612.

Lewis, J.S., Landers, R.J., Underwood, J.C.E., Harris, A.L., and Lewis, C.E. (2000). Expression of vascular endothelial growth factor by macrophages is up-regulated in poorly vascularized areas of breast carcinomas. J. Pathol. *192*, 150–158.

Li, F., Sonveaux, P., Rabbani, Z.N., Liu, S., Yan, B., Huang, Q., Vujaskovic, Z., Dewhirst, M.W., and Li, C.Y. (2007). Regulation of HIF-1α stability through S-nitrosylation. Mol. Cell *26*, 63–74.

Liang, B.C., Thornton, A.F., Jr., Sandler, H.M., and Greenberg, H.S. (1991). Malignant astrocytomas: Focal tumor recurrence after focal external beam radiation therapy. J. Neurosurg. *75*, 559–563.

Lin, E.Y., Nguyen, A.V., Russell, R.G., and Pollard, J.W. (2001). Colony-stimulating factor 1 promotes progression of mammary tumors to malignancy. J. Exp. Med. *193*, 727–740.

Lin, E.Y., Li, J.F., Gnatovskiy, L., Deng, Y., Zhu, L., Grzesik, D.A., Qian, H., Xue, X.N., and Pollard, J.W. (2006). Macrophages regulate the angiogenic switch in a mouse model of breast cancer. Cancer Res. *66*, 11238–11246.

Luo, Y., Zhou, H., Krueger, J., Kaplan, C., Lee, S.H., Dolman, C., Markowitz, D., Wu, W., Liu, C., Reisfeld, R.A., and Xiang, R. (2006). Targeting tumor-associated macrophages as a novel strategy against breast cancer. J. Clin. Invest. *116*, 2132–2141.

Lyden, D., Hattori, K., Dias, S., Costa, C., Blaikie, P., Butros, L., Chadburn, A., Heissig, B., Marks, W., Witte, L., et al. (2001). Impaired recruitment of bone marrow-derived endothelial and hematopoietic precursor cells blocks tumor angiogenesis and growth. Nat. Med. *7*, 1194–1201.

Milas, L., Ito, H., Hunter, N., Jones, S., and Peters, L.J. (1986). Retardation of tumor growth in mice caused by radiation-induced injury of tumor bed stroma: Dependency on tumor type. Cancer Res. *46*, 723–727.

Moeller, B.J., Cao, Y., Li, C.Y., and Dewhirst, M.W. (2004). Radiation activates HIF-1 to regulate vascular radiosensitivity in tumors: Role of reoxygenation, free radicals, and stress granules. Cancer Cell *5*, 429–441.

Moldovan, N.I., Goldschmidt-Clermont, P.J., Parker-Thornburg, J., Shapiro, S.D., and Kolattukudy, P.E. (2000). Contribution of monocytes/macrophages to compensatory neovascularization: The drilling of metalloelastase-positive tunnels in ischemic myocardium. Circ. Res. *87*, 378–384.

Petit, I., Jin, D., and Rafii, S. (2007). The SDF-1-CXCR4 signaling pathway: A molecular hub modulating neo-angiogenesis. Trends Immunol. *28*, 299–307.

Pollard, J.W. (2004). Tumour-educated macrophages promote tumour progression and metastasis. Nat. Rev. Cancer *4*, 71–78.

Rafii, S., Lyden, D., Benezra, R., Hattori, K., and Heissig, B. (2002). Vascular and haematopoietic stem cells: Novel targets for anti-angiogenesis therapy? Nat. Rev. Cancer *2*, 826–835.

Rofstad, E.K., Mathiesen, B., Henriksen, K., Kindem, K., and Galappathi, K. (2005). The tumor bed effect: Increased metastatic dissemination from hypoxia-induced up-regulation of metastasis-promoting gene products. Cancer Res. *65*, 2387–2396.

Rohde, E., Malischnik, C., Thaler, D., Maierhofer, T., Linkesch, W., Lanzer, G., Guelly, C., and Strunk, D. (2006). Blood monocytes mimic endothelial progenitor cells. Stem Cells *24*, 357–367.

Ruzinova, M.B., Schoer, R.A., Gerald, W., Egan, J.E., Pandolfi, P.P., Rafii, S., Manova, K., Mittal, V., and Benezra, R. (2003). Effect of angiogenesis inhibition by Id loss and the contribution of bone-marrow-derived endothelial cells in spontaneous murine tumors. Cancer Cell *4*, 277–289.

Schlaeger, T.M., Bartunkova, S., Lawitts, J.A., Teichmann, G., Risau, W., Deutsch, U., and Sato, T.N. (1997). Uniform vascular-endothelial-cell-specific gene expression in both embryonic and adult transgenic mice. Proc. Natl. Acad. Sci. USA *94*, 3058–3063.

Seandel, M., Noack-Kunnmann, K., Zhu, D., Aimes, R.T., and Quigley, J.P. (2001). Growth factor-induced angiogenesis in vivo requires specific cleavage of fibrillar type I collagen. Blood *97*, 2323–2332.

Semenza, G.L. (2003). Targeting HIF-1 for cancer therapy. Nat. Rev. Cancer *3*, 721–732.

Shaked, Y., Ciarrocchi, A., Franco, M., Lee, C.R., Man, S., Cheung, A.M., Hicklin, D.J., Chaplin, D., Foster, F.S., Benezra, R., and Kerbel, R.S. (2006). Therapy-induced acute recruitment of circulating endothelial progenitor cells to tumors. Science *313*, 1785–1787.

Shekhar, M.P.V., Werdell, J., Santner, S.J., Pauley, R.J., and Tait, L. (2001). Breast stroma plays a dominant regulatory role in breast epithelial growth and differentiation: Implications for tumor development and progression. Cancer Res. *61*, 1320–1326.

Shojaei, F., Wu, X., Malik, A.K., Zhong, C., Baldwin, M.E., Schanz, S., Fuh, G., Gerber, H.-P., and Ferrara, N. (2007). Tumor refractoriness to anti-VEGF treatment is mediated by $CD11b^{+}Gr1^{+}$ myeloid cells. Nat. Biotechnol. *8*, 911–920.

Sica, A., Schioppa, T., Mantovani, A., and Allavena, P. (2006). Tumour-associated macrophages are a distinct M2 polarised population promoting tumour progression: Potential targets of anti-cancer therapy. Eur. J. Cancer *42*, 717–727.

Stoneman, V., Braganza, D., Figg, N., Mercerm, J., Lang, R., Goddard, M., and Bennett, M. (2007). Monocyte/macrophage suppression in CD11b diphtheria toxin receptor transgenic mice differentially affects atherogenesis and established plaques. Circ. Res. *100*, 884–893.

Takahashi, T., Kalka, C., Masuda, H., Chen, D., Silver, M., Kearney, M., Magner, M., Isner, J.M., and Asahara, T. (1999). Ischemia- and cytokine-induced mobilization of bone marrow-derived endothelial progenitor cells for neovascularization. Nat. Med. *5*, 434–438.

Teicher, B.A., Dupuis, N.P., Robinson, M.F., Kusumoto, T., Liu, M., and Menon, K. (1994). Reduced oxygenation in a rat mammary carcinoma post-radiation and reoxygenation with a perflubron emulsion/carbogen breathing. In Vivo *8*, 125–131.

Tsai, J., Makonnen, S., Feldman, M., Sehgal, C.M., Maity, A., and Lee, W.M. (2005). Ionizing radiation inhibits tumor neovascularization by inducing ineffective angiogenesis. Cancer Biol. Ther. *4*, 1395–1400.

Tsai, C.S., Chen, F.H., Wang, C.C., Huang, H.L., Jung, S.M., Wu, C.J., Lee, C.C., McBride, W.H., Chiang, C.S., and Hong, J.H. (2007). Macrophages from irradiated tumors express higher levels of iNOS, arginase-I and COX-2, and promote tumor growth. Int. J. Radiat. Oncol. Biol. Phys. *68*, 499–507.

Twentyman, P.R., Brown, J.M., Gray, J.W., Franko, A.J., Scoles, M.A., and Kallman, R.F. (1980). A new mouse tumor model system (RIF-1) for comparison of end-point studies. J. Natl. Cancer Inst. *64*, 595–604.

Udagawa, T., Birsner, A.E., Wood, M., and D'Amato, R.J. (2007). Chronic suppression of angiogenesis following radiation exposure is independent of hematopoietic reconstitution. Cancer Res. *67*, 2040–2045.

Unsal, D., Uner, A., Akyurek, N., Erpolat, P., Dursun, A., and Pak, Y. (2007). Matrix metalloproteinase-9 expression correlated with tumor response in

patients with locally advanced rectal cancer undergoing preoperative chemoradiotherapy. Int. J. Radiat. Oncol. Biol. Phys. *67*, 196–203.

Yang, L., DeBusk, L.M., Fukuda, K., Fingleton, B., Green-Jarvis, B., Shyr, Y., Matrisian, L.M., Carbone, D.P., and Lin, C. (2004). Expansion of myeloid immune suppressor Gr+CD11b+ cells in tumor-bearing host directly promotes tumor angiogenesis. Cancer Cell *6*, 409–421.

Yu, Q., and Stamenkovic, I. (2000). Cell surface-localized matrix metalloproteinase-9 proteolytically activates TGF-beta and promotes tumor invasion and angiogenesis. Genes Dev. *14*, 163–176.

Zeisberger, S.M., Odermatt, B., Marty, C., Zehnder-Fjallman, A.H., Ballmer-Hofer, K., and Schwendener, R.A. (2006). Clodronate-liposome-mediated depletion of tumour-associated macrophages: A new and highly effective antiangiogenic therapy approach. Br. J. Cancer *95*, 272–281.